Toxicology Reports 6 (2019) 590–597

Contents lists available at ScienceDirect

Toxicology Reports

journal homepage: www.elsevier.com/locate/toxrep

Synthesized Nano particle derivation of poly (Styrene – co- Maleic Anhydride) and sour cherry Rock for removing nickel (II) ion from aqueous solutions

Naser Samadi[a,*], Reza Ansari[b], Bakhtiar Khodavirdilo[b]

[a] Department of Analytical Chemistry, Faculty of Chemistry, Urmia University, Urmia, Iran
[b] Department of Chemistry, Faculty of Science, University of Guilan, University Campus 2, Rasht, Iran

ARTICLE INFO

Keywords:
Adsorbent
Sour cherry rock
Nickel (II) ions
Mechanisms
Melamine-Oxalic acid

ABSTRACT

In this study, Prunus Cerasus Rock (PCR) and Poly (Styrene – co- Maleic Anhydride) modified with Melamine-Oxalic acid (SMA-MO) were used to prepare a cheap adsorbent through chemical modification. The maximum removal was observed at pH = 6.0 and adsorbent dose 1.5 g/L for initial Nickel -ions concentration 30 mg/L. Study of temperature effect proved that the process is endothermic. Langmuir and Freundlich isotherm models were used for equilibrium adsorption data. Langmuir isotherm proved to be a better fit. Pseudo first order and pseudo second order kinetic models were applied to analyze the kinetic mechanism of adsorption.

1. Introduction

Water is one of the most important needs for living in the world. All plants, animals and human must have water to live. It is also necessary for the human activities. Water pollution is increasing worldwide because jumping improvement of industry, increase human population, native and agricultural activities. The elimination of toxic metal ions from wastewaters using various adsorbents has been ever of extensive penchant. So, wastewaters often include remarkable contents of toxic metal ions that would hazard common health and the environment if discharged without enough remedy. High concentrations of the metals in solution effect humans, animals and plant life [1]. Nickel is widely distributed in nature, forming about 0.008% of the earth's crust. The core of the earth contains 8.5% nickel, deep-sea nodules 1.5%; meteorites have been found to contain 5–50% nickel. The natural background levels of nickel in water are relatively low, in open ocean water 0.228–0.693 μg/litre, in fresh water systems generally less than 2.Agricultural soils contain nickel at levels of 3–1000 mg/kg; in 78 forest floor samples from the northeastern United States of America, concentrations of 8.5–15 mg/kg were reported. The nickel content is enriched in coal and crude oil. Nickel in coals ranges up to 300 mg/kg; most samples contain less than 100 mg/kg but there is a large variation by region *(7)*. The nickel content of crude oils is in the range < 1–80 mg/kg. Nickel can be found in drinking-water as a consequence of its presence in alloys used in contact with drinking-water, manganese or Nickel plating of fittings, or its presence in water sources, usually as a consequence of dissolution from naturally occurring Nickel-bearing strata in groundwater. In the first two cases, control is by appropriate control of materials in contact with drinking-water or, in the second instance, education of consumers to flush chromium- or Nickel-plated taps before using the water. Conventional surface water cure, comprising chemical coagulation, sedimentation, and filtration, can achieve 36–82% removal of Nickel. Better Nickel removal occurs with waters containing high concentrations of suspended solids; for waters low in solids, the addition of powdered activated carbon can be used to enhance Nickel removal. In a review of nickel removal, it was concluded that conventional coagulation, clarification, and granular activated carbon filtration can give nickel removals of 36–82%, depending on the speciation of the Nickel. Increasing pH and the presence of high turbidity both favor Nickel removal. The optimum pH for removal of activated carbon was reported to be pH 8. However, other studies have reported that Nickel is rather poorly adsorbed on activated carbon [2]. Absorption can be described as the elimination of toxic heavy metal ions, compounds and ingredients from solution by biological substances and synthesized polymers [3]. Affluent quit of heavy metals into our periphery due to increasing of industrialization and urbanization has introduced an extensive problem universal [4]. Adsorption with bio Sorbent and synthesized polymer is a process that employs economical bio materials and polymers to impound toxic heavy metals and is predominantly advantage for the elimination of contaminants from aqueous environment and industrial effluents. The presence of heavy metals in the aqueous environment is of significant worry due to their

* Corresponding author.
E-mail addresses: samadi76@yahoo.com (N. Samadi), n.samadi@Urmia.ac.ir (B. Khodavirdilo).

https://doi.org/10.1016/j.toxrep.2019.06.008
Received 16 December 2018; Received in revised form 28 May 2019; Accepted 11 June 2019
Available online 12 June 2019

toxicity and health consequence of the human and animals. The non-biodegradable and dangerous nature of the heavy metal pollutants and their attitude to get saved in living organisms is causing a main remedy to environmental tolerability. Nickel is recognized as one of the main heavy metal pollutants cited by electroplating and metal surface remedy industries [5–8]. Nickel reasons Dermatitis, nausea, chronic asthma, human carcinogen and coughing if it is exhibited in access of natural source of water. With the better cognizance of the problems correlated with Nickel came an increase in research investigates associated two methods of removing Nickel from wastewater, an inexpensive and more impressive technology have been improved over the years. Consist adsorption, many methods such as biosorption, precipitation, electrocoagulation, chemical precipitation, membrane filtration, solvent extraction, reverse osmosis and ion exchange [9,10] have been used for the removal of heavy metals from waste water and to modify the quality of the remedy waste water. But in these remedies process adsorption has become one of the significant methods [11,12]. Therefore, in the present study, sour cherry rock sawdust (Prunus Cerasus Rock) (PCR) and poly (Styrene –co- Maleic Anhydride) modified Melamine-Oxalic acid (SMA-MO) have been used to provide a good low cost adsorbent.

2. Experimental methods

2.1. Adsorbents preparation

The Sour cherry rocks applied in this research were prepared from local accessible garden, Urmia, Iran. Pit shells of sour cherry was washed five times with distilled water to eliminate adhesive fruit and dust particles and cut into small pieces, then it was sun dried by exposure to the sunlight for 5 days and subsequently in a hot air convection oven at 110 °C for 24 h. The dried material was ground into a powder using blender and sieved to get constant finer size particles (50 μm). The sieved powder of the raw bio adsorbent (10 g) was imbibed in 0.1 L of 2 N, KOH (Potassium hydroxide) in a mechanical shaker at 220 rpm for 24 h. The activated Sour cherry rock was filtered and leached with distilled water, until the pH was neutral. The base activated bio adsorbent material was sealed in plate and saved in desiccators for further use. The base remedy of bio adsorbent has been done to remove the mineral elements and to increase the basic and hydrophilic nature of the bioadsorbent surface.

2.2. Preparation of CSMA-MO

The Cross-linked Melamine-Oxalic acid functioned SMA polymer (CSMA- MO) was obtained by the simultaneous reaction of the SMA polymer with Melamine-Oxalic acid and 1, 2-diaminoethane (DAE) as the cross-linking agent. The reaction mixture was refluxed for 3 h under inert gas in the presence of ultrasonic irradiation along with vigorous stirring bar in THF. It can be said that the preparation of cross-linked resin in presence of ultrasonic irradiations along with vigorous magnetic stirring give rise polymeric particles in Nano scale. The prepared product was filtered, leached thoroughly with THF, and dried by vacuum oven at 60 °C for 24 h (Scheme1). Maleic anhydride was shown to react rapidly and specifically with amino groups of melamine. Complete substitution of adsorbents was achieved under mild conditions and the extent of reaction could be readily determined from the spectrum of the maleyl-polymer. Maleyl- polymers are generally soluble and disaggregated at neutral pH. Heavy metal ions split the blocked polymer residues and there is frequently selected in this dehydrogenase. The group is removed by intramolecular catalysis at acidic pH.

2.3. Adsorption experiment

The adsorbate reservoir solution of 100 ppm Nickel (II) was obtained from Ni $(NO_3)_2.6H_2O$ in double distilled water. The standard experiment solutions (10–70 ppm) of Nickel (II) were obtained by diluting the reservoir solution as needed by double distilled water. All other chemicals used in this research were purchased from Merck Company. Batch adsorption experiments were performed by shaking 50 mg of adsorbent with 50 ml of Nickel (II) ion solution of the chose concentration at an initial pH of 6.0 in 250 ml conical flasks, which were agitated at 220 rpm and room temperature (25 °C). After a predetermined contact time, the sample was eliminated from the mechanical shaker and filtered by applying Whatman filter paper. The residual concentration of Nickel (II) ions was conjectured by Atomic Absorption Spectroscopy. The influence of concentration (10–60 ppm) of Nickel (II) ions, contact time (0–3 h), adsorbent dose (0.2–3 g/L) and pH (2–10) were looking in a batch adsorption experiment. The optimum condition (pH 6.0, contact time 90 min, adsorbent dose 1.5 g/L of 100 ml) for adsorption isotherm was fixed. The amount of Nickel -ions adsorbed (q_e) from aqueous solution and percentage elimination of Nickel-ions were computed by using the following Equations (1) and (2) respectively.

$$q_e = \frac{(C_o - C_e)V}{w} \quad (1)$$

$$R\,\% = \frac{(C_o - C_e)}{C_o} \times 100 \quad (2)$$

Where C_o and C_e is the initial and the equilibrium concentration (mg/L) of the Nickel (II) ion solution, V is the volume of Nickel (II) ion solution in L, m is the mass of adsorbent in grams [13].

2.3.1. Characteristic techniques

The PCR and CSMA-MO were characterized by applying a BET technique (BEL Japan) to measure surface area. SEM (scanning electron microscope) applied to measure the surface morphology of PCR and CSMA-MO. The FT-IR spectra of PCR and CSMA-MO before and after adsorption of Nickel-ions were prepared to represent the functional groups on the surface.

3. Results and discussion

3.1. Characterization of the adsorbents

The BET technique was applied to measure surface area and pore size of the PCR and CAMA-MO. The BET surface area of PCR and CAMA-MO is 4.7422 and 4.680 m^2/mg and mean pore diameter is 2.7011and 2.67 nm respectively. The Nano sheet morphology of PCR and CAMA-MO tested by SEM is exhibited in Fig. 1. The erratic and porous structures with external of adsorbent play a significant role in adsorption [14]. A Fourier transform infrared spectrum (FTIR) was applied to investigate the changes in vibrational frequency in the functional groups of the adsorbents to Nickel (II) adsorption. The adsorbent was scanned in the spectral range of 400-4000 cm^{-1}. The Fig. 4 represents the FTIR spectra of CAMA-MO before and after adsorption. Figs. 2–4 exhibits the FTIR plot of CSMA-MO and PCR. The broad and strong bands at about3430 cm^{-1} were to bonded hydroxyl (−OH) or amine groups (-NH) of the CSMA-MO and PCR respectively. The peak at about 1610 cm^{-1} is attributed to the carboxyl group (-C = O) stretching vibration. The peak at about 1745 cm^{-1} for stretching of C–O bonds in carboxylic acid and ester components and about 1342 cm^{-1} for C–O stretching in the acetyl groups in hemicelluloses in PCR. It was later reported that these functional groups in CSMA-MO and PCR are able of adsorbing different heavy metal ions. The spectra indicated a number of changes in peaks, which exhibit the complex nature of the adsorbent. The functional group is one of the key factors to carry out the mechanism of the Nickel binding process on natural adsorbents. The shifts in the wavelength exhibited that there was a Nickel binding process taking place at the surface of the PCR and CAMA-MO [15]. The adsorption of Ni^{2+} ion on the adsorbents were more favorable at

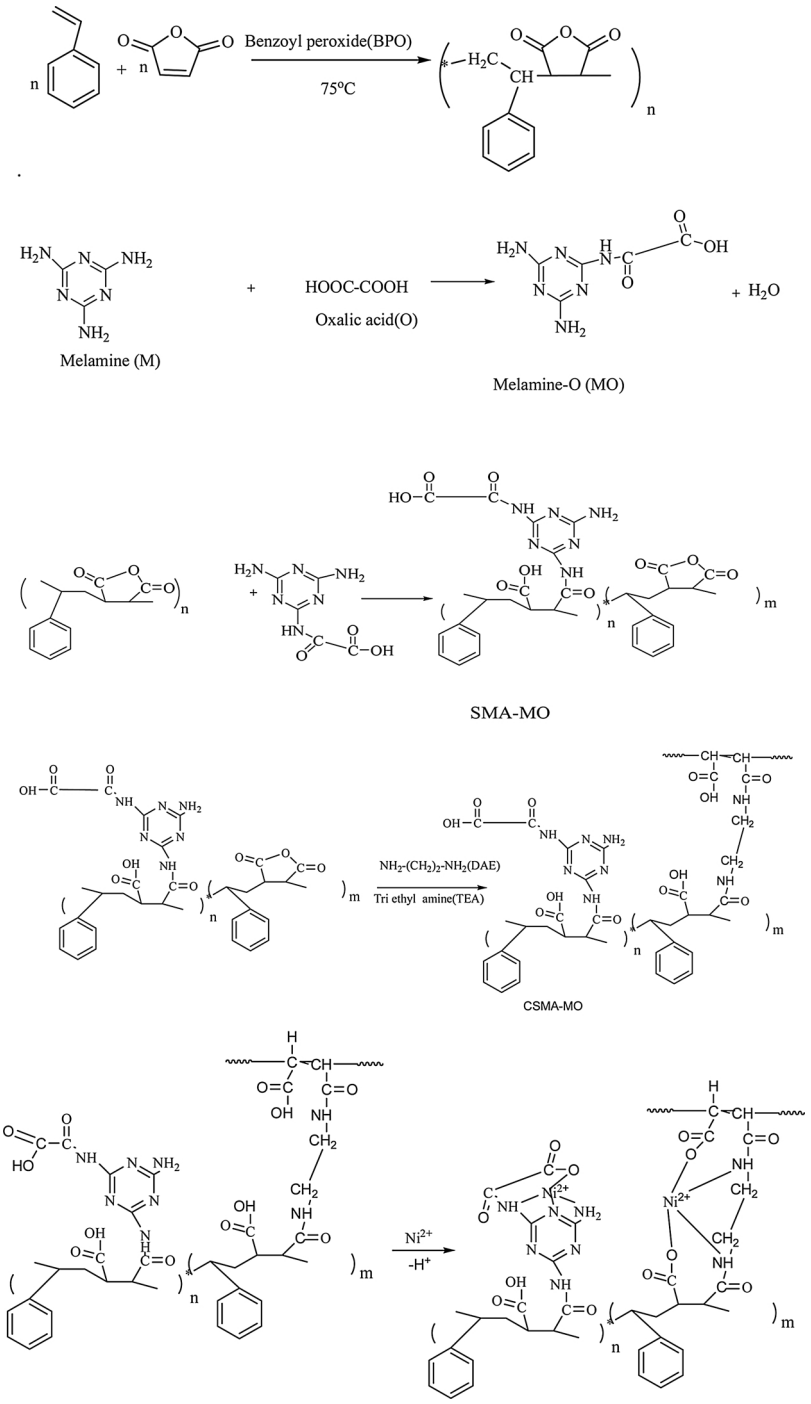

Scheme 1. Structure of polymer (SMA) and its derivations.

pH = 6. At low pH value a high concentration of H^+ could react with Carboxylate ions (COO -) and Amine groups in CSMA-MO and Hydroxyl groups in PCR to form protonation. In other word, H^+ could compete with Nickel (II) ions for adsorption sites and reduce the Nickel (II) ion adsorption capacity. At the Alkaline pH value, the Nickel (II) ions could be precipitated by OH- to form Ni $(OH)_2$, instead of adsorbent- Ni (II) ion complexation. So, pH = 6 was optimized pH for removal of Ni (II) ions from aqueous solution. The shift of infrared adsorption bonds for the free Carbonyl bond (C═O) of the Carboxylate groups illustrated whether the bonding between the ligand and Nickel (II) ions in the solid phase was covalent or ionic. The more covalent it was the higher the frequency shift was for the free Carbonyl bond adsorption. In this study the adsorption bond for C═O in the chelating group shifted to higher frequencies with increasing covalent nature of the Carbonyl bond in the results of complexation with ionic Nickel(II) ion and appeared about 1695-1715 cm^{-1} It was interesting that the absorption peaks at about 1715 cm^{-1}. That bonds at 1635, 1565, 1459 and 1249 cm^{-1} shifted to a lower frequency ; this indicated that the Nickel(II) ion coordination through the chelating ligands was done in the polymer network also, the absorption bonds characteristic of the atomic parts of the matrix (1035, 918, 768 and 708 cm^{-1})were not influenced by the Ni (II)ion complexation. The scale bar for PCR and CSMA-MO are 500 and100 nm respectively. Fig. 1 shows the SEM micrographs of typical SMA-MO and PCR, in which the particles processed an almost uniform. Distribution of sizes is with spherical shapes. The diameter of the observed particles in the SEM images was estimated to be less than 100 nm [16].

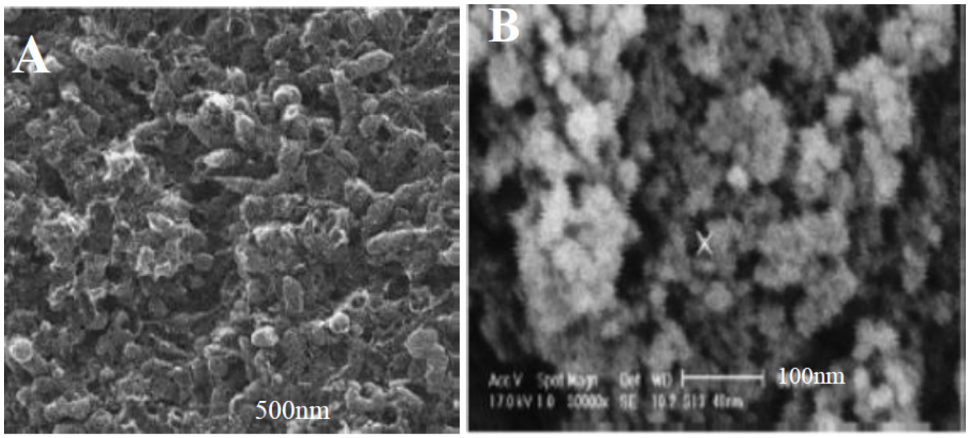

Fig. 1. SEM image of Sour Cherry Rock (PCR) (scale = 500 nm) (A) and CSMA-MO (scale = 100 nm) (B).

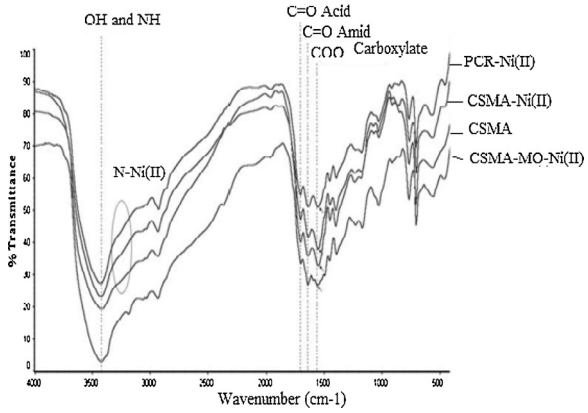

Fig. 2. FT-IR spectrum of the Iranian pit shells (Sour Cherry rock) (PCR), SMA and modified SMA as adsorbents for removing Nickel (II) ions from aqueous solution.

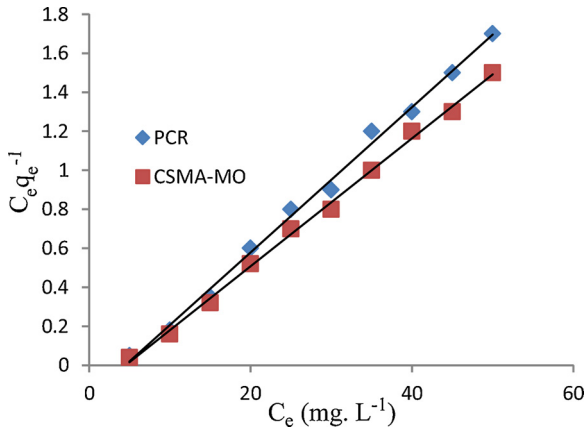

Fig. 3. Langmuir isotherm for elimination of Nickel (II) ion adsorption on PCR and CSMA-MO.

Some peaks of (−OH) groups in Carboxyl of CSMA-MO and acidic (−OH) in PCR were disappeared by adsorbents. If the number of Amine and Carboxyl groups increase, The probability of forming ionic and dative bond between Ni^{2+} ions, Carboxylate and Amine groups and removal of Ni^{2+} ions from aqueous solutions will increase too.

3.2. Effect of pH on adsorption

The pH is one of the most significant performing variables in the adsorption process since the amounts of pH affect the surface and binding capacity of adsorbent due to exchange of H^+ ions with Nickel (II) ions. The effect of pH on the adsorption of Nickel (II) ions by CSMA-MO and PCR were investigated at pH 2.0–10 (Table 1). The results show maximum adsorption pH = 6.0. So, residual tests were understood on this pH. Lower amount of pH favor the adsorption, but with increase in pH from 6.0 to 8.0, the elimination percentage decreased. The adsorption of Nickel (II) ions increased with increasing pH and reached a limiting value in each instance, which was followed by a decrease in adsorption beyond the limiting value. It is well known that the adsorption of Nickel (II) ions by adsorbents depends on the pH: These affect the chelation extremely as well as the physic sorption process, thus, the effect of pH on the adsorption capacities needed to be further investigated. The CSMA-MO resin was dissolved completely in water at pH = 8.5 because of its noncrosslinked nature, and its hydrophilicity was increased because of the deporotonation of its functional group. The effect of crosslinking on the sorption revealed that the sorption capacity increased in the crosslinked sample by 1,2 diaminoethane compared to that in the noncrosslinked sample. There was an abrupt increase in the Ni (II) ion adsorption when the pH was raised from 2 to 10. The results indicate that with increasing pH from 2 to 6, the adsorption percentage increased for Ni^{2+} and It remained nearly unchanged from pH = 6 to pH = 10.

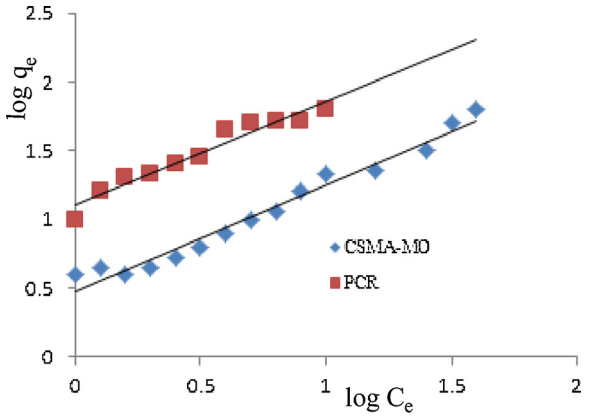

Fig. 4. Freundlich isotherm for elimination of Nickel (II) ion adsorption on PCR and CSMA-MO.

3.3. Effect of adsorbent dosage

Adsorbent dose is a significant factor since it measures the binding capacity of adsorbent for obtained initial Nickel (II) ion concentration. The Table 1 represents the elimination of Nickel (II) ions as an

Table 1
Optimized conditions for removing Nickel (II) ions from aqueous solutions.

Characters	Removal percentage	
pH	PCR	SMA-MO
1	10	12
2	38	40
3	60	48.2
4	82	89
5	90.3	98.4
6	99.3	99.7
8	99.2	99
10	99.1	98.9
Adsorbent dose (g L^{-1})		
0	0	0
0.25	60	70
0.5	75	82
0.75	85	87
1	95.2	97.6
1.25	97.1	98.3
1.5	99.2	99.6
2	99	99.4
2.5	98.1	98.7
3	98.2	98.6
Initial Nickel (II) ion concentrations(mg L^{-1})		
10	90	92
15	92.1	93.3
20	93.1	94.2
25	94.8	96.4
30	95.1	97.2
35	96.1	98.2
40	97.1	99.1
45	98.1	99.4
50	99.5	99.7
55	99.1	99
60	99.1	99.2
70	98.1	97.3
Contact time (min)		
0	0	0
20	45	48.2
40	50	55.2
60	70	75
70	80	84.6
80	95.6	98.2
90	99.3	99.8
100	99.3	99.8
120	99.2	99.7
150	98.2	98.9

operation of CSMA-MO and PCR added to an aqueous solution of pH = 6.0. CSMA-MO and PCR snippet dose confined from 0.2 to 3.0 g/L of Nickel (II) ions experiment solution and was equilibrated for 90 min while keeping other parameters at optimal. The percentage Nickel (II) ions elimination was 99.2% (at 1.5 g/L of adsorbent dosage) and increased to 98.8781% (at5 g/L of adsorbent dosage). Increase in removal percentages with increasing CSMA-MO and PCR dosage is depended on to the increase in external area and by propagation the accessed number of ion replaceable sites accessible for interaction with Nickel (II) ions. The decrease in Nickel (II) ions adsorbed (mg/g) with an increase in adsorbent dose is due to the increase in surface sunken site. The test results exhibit that optimal adsorbent dosage was 1.5 g/L for this test [17].

3.4. Effect of initial Nickel (II) ion concentration

Nickel (II) ions adsorption on CSMA-MO and PCR were investigated, using various initial Nickel (II) ion concentrations in the range of 0–70 mg/L at optimal conditions of contact time (90 min), temperature (25 °C), pH = 6 and adsorbent dosage (1.5 g/L). It was leaked that the elimination of Nickel (II) ions decreases with increase in initial Nickel (II) ion concentration of Nickel (II) ions (Table 1) [18]

3.5. Effect of contact time

The adsorption of Nickel (II) ions from aqueous solution on CSMA-MO and PCR increases with increase in contact time. It was leaked that the common uptake rate was fast during the first 1.5 h, after which adsorption was arrived at steady state. The Table 1 represents the effect of contact time on the CSMA-MO and PCR elimination of 50 mg/L Nickel (II) ions at 25 °C and pH 6.0. The initial uptake rate was fast during first 1 h may be due to the mere accessibility of the surface vacuous sites. Two kinetic models, Lagergren first-order and Ho's second-order was used to analyze the adsorption rates of Nickel (II) ions onto the CSMA-MO and PCR [19,20].

3.6. Adsorption isotherms

Adsorption isotherms explain the remedy of adsorption process and the interaction of the adsorbate with the adsorbent. In this research, two adsorption isotherms, Langmuir and Freundlich, were applied for matching the prepared tentative adsorption data.

3.6.1. Langmuir isotherm

Adsorption isotherms are significant for the explanation of how sorbate will interact with a Sorbent and climacteric in modifying the use of adsorbent [21]. These adsorption model parameter amounts of these two equilibrium adsorption models are measured [22]. The Langmuir model introduces one of the first theoretical remedies of non-linear sorption and offers that uptake happens on a homogenous external by monolayer sorption without effect between adsorbed molecules. The Langmuir isotherm describes monolayer adsorption, linearized model of the Langmuir isotherm can be exhibited by the following Eq. (3) [23–25].

$$q_e = \frac{q_{max} C_e K_L}{1 + K_L C_e} \tag{3}$$

Lined equation :

$$\frac{C_e}{q_e} = \frac{1}{q_{max} K_L} + \frac{C_e}{q_{max}} \tag{4}$$

Where, the equilibrium concentration is C_e (mg/L), the value of Nickel (II) ion adsorbed per unit weight of adsorbent at equilibrium is q_e (mg/g), q_{max} is the theoretical maximum adsorption capacity (mg/g), K_L is the Langmuir isotherm constant (L/mg). The amount of R^2, K_L and q_{max} were measured from the slopes and amputates of the linear plots of C_e/q_e versus C_e (Table 2 and Fig. 3).

3.6.2. Freundlich isotherm

Freundlich isotherm describes heterogeneous surfaces and multilayer adsorption, the linearized model of Freundlich isotherm can be exhibited by the following Eq. (5).

$$\mathrm{Log}\, q_e = \mathrm{Log} K_F + \frac{1}{n} \mathrm{Log} C_e \tag{5}$$

Where, K_F is the Freundlich adsorption constant associated with the adsorption capacity of the adsorbent (mg/g) (mg/L). 1/n and n are dimensionless constants of the adsorbents, which can be applied to describe the adsorption severity between the solved concentration and

Table 2
Langmuir and friendlier isotherm constants for the adsorption of Nickel (II) ion onto PCR and CSMA-MO.

Langmuir Isotherm	CSMA-MO	PCR	FreundlichIsotherm	CSMA-MO	PCR
q_{max} (mg/g)	84.03	79.3	n	1.29	1.33
K_L(L/mg)	0.25	0.26	K_F (mg/g)	3	12.62
R^2	0.9942	09927	R^2	0.9716	0.9472

Table 3
Comparison of adsorption capacity q_{max} (mg. g^{-1}) Nickel (II) ion onto different adsorbents.

Adsorbent	q_{max} (mg. g^{-1})	Reference
Amberlite IRC-748	62.20	36
IRN-77	62.11	37
CT-BHQbeads	9	38
Tea factory waste	15.26	34
Eutrophic peat	11.15	35
Banana peel	6.88	33
PCR	79.3	This study
CSMA-MO	84.03	This study

Table 4
Pseudo first-order and pseudo second-order reaction rate constants for Nickel (II) on adsorption by PCR and CSMA- MO adsorbents.

	PCR	CSMA- MO
Pseudo first-order		
Equation Regression	Y= - 0.012x +1.8024	Y= - 0.0171x +2.0269
k_1 (min^{-1})	0.028	0.039
R^2	0.9817	0.9894
Pseudo second order		
Equation Regression	Y= 0.0091x +0.3603	Y= 0.0097x +0.147
k_2 (g/mg·min)	2.3×10^{-4}	6.4×10^{-4}
R^2	0.9978	0.9996

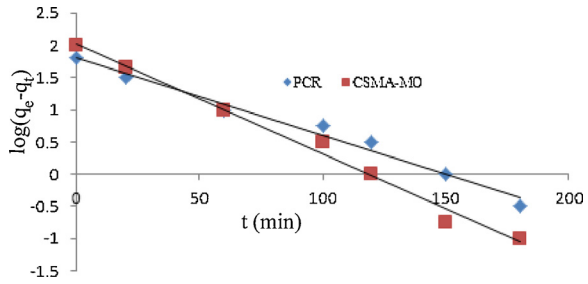

Fig. 5. Pseudo first order kinetics.

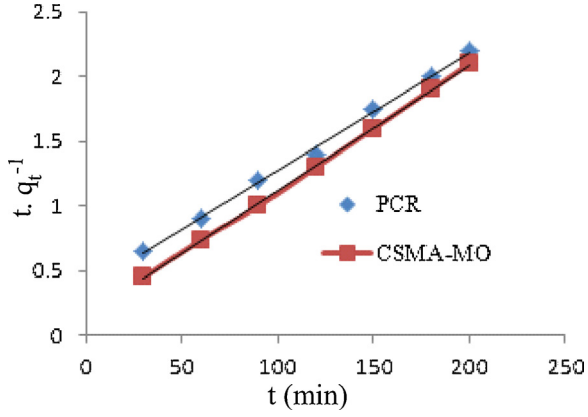

Fig. 6. Pseudo second order kinetics.

adsorbent respectively. The amount of R^2, K_F and n were measured from the slopes and amputates of the linear plots of Log q_e versus Log C_e (Table2 and Fig. 4) [26–28].

The maximum values of Nickel ions adsorbed (q_{max}) onto CSMA-MO and PCR were found to be 84.03 and 79.3 mg g^{-1} for Ni^{2+} ions respectively. The amount of K_L for Ni^{2+} with CSMA-MO and PCR was 0.25 and 0.26 L mg^{-1} respectively. The usability of the Langmuir isotherm to the adsorption of Ni^{2+} ions onto CSMA-MO and PCR predicted high correlation coefficients (R^2 > 0.99) compared to Freundlich

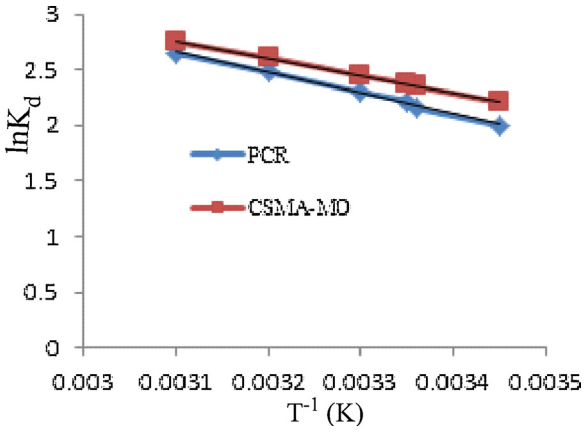

Fig. 7. The influence of temperatures on the adsorption of Nickel (II) ion onto PCR and CSMA-MO.

isotherm (Table 2) and our adsorbents were compared with the other adsorbents in table 3 (Table 3).

3.7. Kinetic studies

In this work, the Lagergren first-order reaction rate model (pseudo-first order adsorption kinetics, Eq. (6) and Ho's second order reaction rate model (pseudo-second order adsorption kinetics, Eq. (7) has been used to the experimental data to measure the adsorption kinetics of Nickel(II) ions.

$$log\,(q_e - q_t) = log q_e - \frac{K_1 t}{2.303} \quad (6)$$

$$\frac{t}{q_t} = \frac{1}{K_2 q_e^2} + \frac{1}{q_e} t \quad (7)$$

Where, the maximum adsorption capacity at equilibrium is q_e (mg/g) and the value of Nickel (II) -ion adsorbed at time, t is q_t (mg/g). k_1 (min^{-1}), k_2 (g/mg min) is the equilibrium rate constants for pseudo-first order and pseudo-second order kinetics respectively. The Results of the kinetic data indicated that the pseudo-second order model best explains the adsorption of Nickel (II) on PCR and CSMA- MO. The R^2 value of the pseudo second order was higher than that of pseudo first order kinetic model (Table 4) [29,30].

3.8. Thermodynamic studies

The influence of temperatures on the adsorption of Nickel (II) ion onto PCR and CSMA-MO surface has been exhibited in Figs. 5 and 6. The curve presents light increment in adsorption on the increment in temperature. This perhaps the reason a vaster kinetic energy gained by the Nickel (II) ions with increment in temperature. The cohesion of standard Gibbs free energy (ΔG°) and thermodynamic equilibrium constant kid can be remarked by following equation [31,32].

$$\Delta G = - RTLn\ K_d \quad (8)$$

Adsorption enthalpy (ΔH°), and adsorption entropy (ΔS°), depends on the standard Gibbs free energy (ΔG°) exhibited by Van't Hoff equation, presented in Eq. (9).

$$Ln\ Kd = -\frac{\Delta G^o}{RT} = -\frac{\Delta H^o}{RT} + \frac{\Delta S^o}{R} \quad (9)$$

K_d is exhibited by the Eq. (10).

$$Kd = \frac{C_A}{C_E} \quad (10)$$

Where: C_A is the value of Nickel (II) ions adsorbed at equilibrium and C_E

Table 5
Thermodynamic characters for the adsorption of Nickel (II) ion from aqueous solution onto PCR and CSMA-MO.

Temperature (K)		LnK_d	ΔG° (Kj·mol^{-1})	ΔH° (Kj·mol^{-1})	ΔS° (j· mol^{-1})	R^2
PCR	290	2.012	−4.85	15.40	69.94	0.9954
	293	2.161	−5.26			
	298	2.223	−5.50			
	303	2.332	−5.85			
	313	2.483	−6.45			
	323	2.542	−6.75			
CSMA-MO	290	2.211	−5.35	12.86	62.79	0.9986
	293	2.352	−5.54			
	298	2.382	−5.86			
	303	2.454	−6.17			
	313	2.612	−6.80			
	323	2.750	−7.43			

is the equilibrium concentration. The amounts of ΔH° and ΔS° were computed from the slope and amputate of the plot (Ln K_d against 1/T Fig. 7) and the computed thermodynamic parameter amounts are exhibited in Table 5. The ΔS°, ΔH° and ΔG° produce the entropy, enthalpy and free energy changes during the process of adsorption in this work, respectively [33–36]. The positive value of ΔH° confirms endothermic feature of adsorption for the system at hand. Because, the positive amount of ΔS° remarks the raised factor of randomness at the solid/solution media amounts the adsorption of Nickel (II) on PCR and CSMA-MO. The negative amounts of ΔG° at all temperatures as represented in Table 5 represent a spontaneous feature of adsorptions.

3.9. Desorption and repeated use

Desorption of Nickel (II) ions was administered by 0.2 N HNO_3 solutions. The CSMA-MO– Nickel (II) ions and PCR- Nickel (II) ion complexes were imbibed in 0.2 N HNO_3 solution and the mixture were shaken until equilibrium was arrived (45 min). Then the mixture was filtrated and the final concentrations of Nickel (II) ions in the aqueous solution were measured by AAS. The desorption ratio (D%) of Nickel (II) ions from the CSMA-MO and PCR was computed with the following equation:

$$D\ \%= \frac{C_a\ V_a}{(C_o\ -\ C_e)V} \times\ 100 \qquad (10)$$

Where V is the volume of the solution (L); C_a is the concentration of the Nickel (II) ions in the desorption solutions (mg/L), and V_a is the volume of the desorption solution (L). Desorption of Nickel (II) ion from The CSMA-MO– Nickel (II) ion and PCR- Nickel (II) ion complexes are 99% and 98.5%, respectively [37–42]. The raked CSMA-MO and PCR from the desorption process was leached thoroughly with deionized water and dried by vacuum pump at 65 °C for reuse [43–45].

4. Conclusions

This work successfully explained the using of modified PCR and CSMA-MO as a low cost adsorbent and suitable for the removal of Nickel (II) ions from aqueous solutions. An increment in pH was remarkable up to 6.0 where an increment in adsorbent dosage resulted in raising elimination efficiencies and reduced uptake capacities. The Langmuir isotherm was illustrated to ready the best match for the equilibrium adsorption data corroborating a monolayer adsorption plot. The pseudo-second order model matched well with the kinetic data this study presents a slight increment in adsorption on the increase in temperature. This perhaps the reason a vaster kinetic energy gained by the Nickel (II) ions with increment in temperature, contact time is short and the amount of adsorbent dosage is low. From this work, we deduce that activated PCR powder and modified SMA with melamine-oxalic acid can be applied as adsorbent for the elimination of Nickel (II) ions from aqueous solution. Maximum adsorption (q_{max}) of CSMA- MO is more than PCR. So, these adsorbents are very suitable for removing Nickel (II) ions from aqueous solution.

Declaration of Competing Interest

We would like to research about removal heavy metal ions from aqueous solutions by using inexpensive adsorbents.

Acknowledgements

The authors would like to thank Samaneh Khodavirdilo Doctor of veterinary medicine for typing and the other works of computer and translation. The authors thank Urmia university polymer laboratory for preparing polymers.

References

[1] V.V. Chernyshev, et al., Morphologic and chemical composition of particulate matter in motorcycle engine exhaust, Toxicol. Rep. 5 (2018) 224–230.
[2] S. Khan, Q. Cao, Y.M. Zheng, Y.Z. Huang, Y.G. Zhu, Environ. Pollut. 152 (2008) 686–692.
[3] A. Singh, R.K. Sharma, M. Agrawal, F.M. Marshall, Food Chem. Toxicol. 48 (2010) 611–619.
[4] S.H. Peng, W.X. Wang, X.D. Li, Y.F. Yen, Chemosphere 57 (2004) 839–851.
[5] World Health Organization, 2nd ed., Guidelines for Drinking- Water Quality Volume 1 World Health Organization, Geneva, 1998.
[6] F.L. Fu, Q. Wang, J. Environ. Manage. 92 (2011) 407–418.
[7] Y.H. Wang, S.H. Lin, R.S. Juang, J. Hazard. Mater. 102 (2003) 291–302.
[8] D.W. O'Connell, C. Birkinshaw, T.F. O'Dwyer, Bioresour.Technol. 99 (2008) 6709–6724.
[9] T.A. Kurniawan, G.Y.S. Chan, W.H. Lo, S. Babel, J. Chem.Eng. 118 (2006) 83–98.
[10] J.M. Antonini, et al., Aerosol characterization and pulmonary responses in rats after short-term inhalation of fumes generated during resistance spot welding of galvanized steel, Toxicol. Rep. 4 (2017) 123–133.
[11] F.Y.A. El Kady, M.G. Abd El, S. Wahed, A.O. Shaban, J. Abo El Naga, Fuel 89 (2010) 3193–3206.
[12] K. Kadirvelu, C. Namasivayam, Adv. Environ. Res. 7 (2003) 471–478.
[13] B. Muhammad Ibrahim, WahabL.O. Jimoh, Int. J. Biol Chem. Sci. 5 (3) (2011) 915–922.
[14] Y. Feng, J.-L. Gong, G.-M. Zeng, Q.-Y. Niu, H.-Y. Zhang, C.-G. Niu, J.-H. Deng, M. Yan, Chem. Eng. J. 162 (2010) 487–494.
[15] M.M. Rao, A. Ramesh, G.P.C. Rao, K. Seshaiah, J. Hazard. Mater. B129 (2006) 123–129.
[16] F.I. Abdel Samea, S.A. Shaban, N.A. Yussef, M.M. Selim, Egypt. J. Pet. 19 (2010) 1.
[17] O.A. Fadali, E.E. Ebrahiem, Y.H. Magdy, A.A. Daifullah, M. Nassar, J. Environ. Sci. Health Part A Environ. Sci. Eng. 9 (2005) 465–472.
[18] C. Rusov, R. Zivkovic, L. Jojic-Malicevic, Acta Vet. (Beogr) 47 (1997) 371–376.
[19] I.H. Scheinberg, I. Sternleib, Am. J. Clin. Nutr. 63 (1996) 842S–845S.
[20] W. Seffner, Toxicol. Lett. 92 (1996) 161–172.
[21] S.F. Taghizadeh, et al., Health risk assessment of heavy metals via dietary intake of five pistachio (Pistacia Vera L.) cultivars collected from different geographical sites of Iran, Food Chem. Toxicol. 107 (2017) 99–107.
[22] Ya.O. Mezhuev, et al., Effect of Poly(ethylene oxide) on the Kinetics of Oxidative Polymerization of Aniline // Russian, J.General Chem. 86 (2016) 2520–2525.
[23] W. Stumm, J.J. Morgan, Aquatic Chemistry, Wiley Interscience, New York, 1996.
[24] O. Ya, O. Mezhuev Ya, et al., Oxidative polymerization of aromatic amines: kinetic trends and possible mechanisms //, Russ. Chem. Rev. 86 (2017) 1271–1285.
[25] M.J. McCoy, et al., Diacetyl and 2,3-pentanedione in breathing zone and area air during large-scale commercial coffee roasting, blending and grinding processes, Toxicol. Rep. 4 (2017) 113–122.

[26] Ya.O. Mezhuev, et al., A new concept of the kinetics and mechanism of the oxidative polymerization of aromatic amines, Russ. J. Phys. Chem. B 9 (2015) 306–315.
[27] I.L. Hsiao, Y.J. Huang, Effects of various physicochemical characteristics on the toxicities of ZnO and TiO2 nanoparticles toward human lung epithelial cells, Sci.Total Environ. 409 (7) (2011) 1219–1228.
[28] A.Y.P. Wardoyo, U.P. Juswono, J.A.E. Noor, Varied dose exposures to ultrafine articles in the motorcycle smoke cause kidney cell damages in male mice, Toxicol. Rep. 5 (2018) 383–389.
[29] A. Seco, J. Chem. Tech & Biotech. 68 (1997) 23–30.
[30] Y. Yamada, et al., Comparison of the neurotoxicities between volatile organic compounds and fragrant organic compounds on human neuroblastoma SK-N-SH cells and primary cultured rat neurons, Toxicol. Rep. 2 (2015) 729–736.
[31] C. Gao, Z. He, J. Li, X. Li, Q. Bai, Z. Zhang, Z. Zhang, S. Wang, X. Xiao, F. Wang, Y. Yan, D. Li, L. Chen, X. Zeng, Y. Xiao, G. Dong, Y. Zheng, Q. Wang, W. Chen, Specific long non-coding RNAs response to occupational PAHs exposure in coke oven workers, Toxicol. Rep. 3 (2016) 160–166.
[32] S. Babel, T.A. Kurniawan, A review, J. Hazard Mater. B. 97 (2003) 219–243.
[33] S. Liang, X. Guo, Q. Tian, Desalin, 11Water Treat. 51 (2013) 7166–7171.
[34] R.M. Schneider, C.F. Cavalin, M.A. Barros, C.R.G. Tavares, Chem. Eng. J. 132 (2007) 355–362.
[35] A. Kosak, A. Lobnik, M. Bauman, Int. J. Appl. Ceramic Tech. 12 (2015) 461–472.
[36] I. Tongo, O. Ogbeide, L. Ezemonye, Human health risk assessment of polycyclic aromatic hydrocarbons (PAHs) in smoked fish species from markets in Southern Nigeria, Toxicol. Rep. 4 (2017) 55–61.
[37] K. Bhattacharya, T.K. Naiya, S.N. Mandal, S.K. Das, Chem. Eng. J. 137 (2008) 529–542.
[38] O.E. Orisakwe, Z.N. Igweze, K.O. Okolo, N.A. Udowelle, Human health hazards ofpoly aromatic hydrocarbons in Nigerian smokeless tobacco, Toxicol. Rep. 2 (2015) 1019–1023.
[39] N. Samadi, R. Ansari, B. Khodavirdilo Euras, J. Anal. Chem. 13 (2018) 1–20.
[40] Y.L. Chen, X.Q. Hong, H. He, H.W. Luo, T.T. Qian, Bioresour. Technol. Rep. 160 (2014) 89–92.
[41] X. Lv, G. Jiang, X. Xue, D. Wu, T.S.C. Sun, J. Hazard. Mater. 262 (2013) 748–758.
[42] H. Xu, Z. Yang, Z.G. Ming, Y. Luo, J. Huang, Chem. Eng. J 239 (2014) 132–140.
[43] M.S. Oncel, A. Muhcu, E. Demirbas, M. Kobya, J. Environ,Chem,Eng 1 (2013) 989–995.
[44] L. Zhou, Z. Zhang, W. Jiang, W. Guo, H. Ngo, j, Bioadhesion and Biofilm Res. 30 (2014) 105–114.
[45] S.W. Ali, F.W.M.A. Malik, T. Yasin, B. Muhammad, J. Appl. Polym. Sci. 129 (2013) 2234–2243.